

Electrical conductivity of orthopyroxene: Implications for the water content of the asthenosphere

By Lidong DAI^{*1,*2} and Shun-ichiro KARATO^{*2,†}

(Communicated by Ikuo KUSHIRO, M.J.A.)

Abstract: Electrical conductivity of minerals is sensitive to water content and hence can be used to infer the water content in the mantle. However, previous studies to infer the water content in the upper mantle were based on pure olivine model of the upper mantle. Influence of other minerals particularly that of orthopyroxene needs to be included to obtain a better estimate of water content in view of the high water solubility in this mineral. Here we report new results of electrical conductivity measurements on orthopyroxene, and apply these results to estimate the water content of the upper mantle of Earth. We found that the electrical conductivity of orthopyroxene is enhanced by the addition of water in a similar way as other minerals such as olivine and pyrope garnet. Using these new results, we calculate the electrical conductivity of pyrolite mantle as a function of water content and temperature incorporating the temperature and water fugacity-dependent hydrogen partitioning. Reported values of asthenosphere conductivity of $4 \times 10^{-2} - 10^{-1}$ S/m corresponds to the water content of 0.01–0.04 wt%, a result in good agreement with the petrological model of the upper mantle.

Keywords: electrical conductivity, orthopyroxene, water, asthenosphere

Introduction

It was proposed that water (hydrogen) may enhance electrical conductivity of minerals¹⁾. If it is the case, then much of the electrical conductivity in Earth's mantle is due to proton (hydrogen) but not by "polaron" (ferric iron to ferrous iron hopping) as previously considered^{2)–4)} and electrical conductivity might be used to infer the water content in Earth's interior. Consequently, a large number of experimental studies have been conducted to study the influence of water (hydrogen) on the electrical conductivity of mantle minerals^{5)–10)}. For example, Wang *et al.*¹⁰⁾ determined the influence of water on conductivity of olivine and inferred the water content of Earth's upper mantle. A similar study was conducted by Yoshino *et al.*⁵⁾ who obtained different conclusions on the influence of water from those by Wang *et al.*¹⁰⁾.

Karato and Dai¹¹⁾ and Dai and Karato⁸⁾ showed that the discrepancies between the results from these two laboratories are due to the technical problems in the approach by Yoshino *et al.*⁵⁾ (see also references^{6),12)}), and after the correction of technical problems in Yoshino *et al.*⁵⁾, most of the published results agree each other.

However, even though these technical problems have been resolved¹¹⁾, the previous studies are incomplete because they considered olivine only in estimating the water content of the upper mantle. The recent study by Mierdel *et al.*¹³⁾ showed that orthopyroxene can dissolve a significantly higher amount of water than olivine under the shallow upper mantle conditions, implying that orthopyroxene might have important effects on electrical conductivity of the upper mantle. However, until now, no data have been reported on the conductivity of hydrous pyroxene, which constitutes about 20–40% of the minerals in the upper mantle. Another issue is the water content measurements. In most cases, water content in minerals is measured either by FT-IR (Fourier-transformed infrared spectroscopy) or SIMS (secondary ion mass spectrometry), but SIMS gives a factor of ~ 3 higher water content than FT-IR for olivine (there is no

^{*1} Laboratory for Study of the Earth's Interior and Geofluids, Institute of Geochemistry, Chinese Academy of Sciences, Guiyang, China.

^{*2} Department of Geology and Geophysics, Yale University, New Haven, USA.

[†] Correspondence should be addressed: S. Karato, Department of Geology and Geophysics, Yale University, New Haven, CT 06511, USA (e-mail: shun-ichiro.karato@yale.edu).

Table 1. Chemical composition of the samples (wt%)

	Cr ₂ O ₃	NiO	MnO	FeO	Na ₂ O	K ₂ O	Al ₂ O ₃	CaO	MgO	TiO ₂	SiO ₂
Sample A	0.37	0.01	0.26	9.12	0.07	0.02	0.79	0.36	32.14	0.09	56.77
Sample B	0.92	0.08	0.34	11.73	0.01	0.03	0.42	0.51	30.48	0.05	55.43

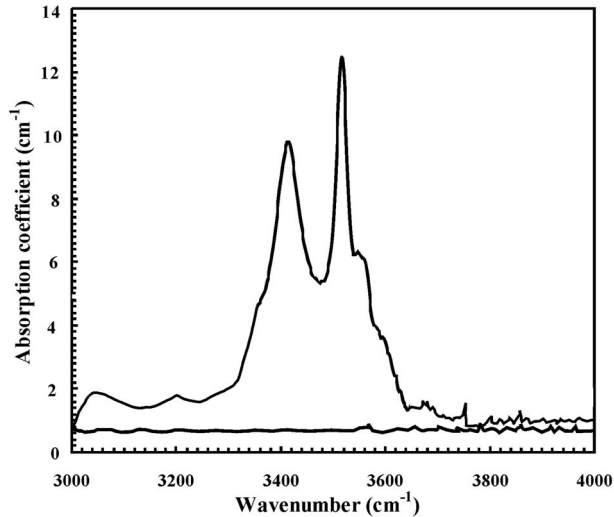


Fig. 1. FT-IR spectra of hydrous and dry orthopyroxene (beam parallel to [001]) for the wavenumber range from 3000 to 4000 cm⁻¹. For a hydrous sample, well-defined absorption peaks are observed at 3064, 3415 and 3515 cm⁻¹, and the total water content of the crystal is ~4650 ppm H/Si (0.042 wt%) and the water content of an anhydrous sample is less than 8 ppm H/Si.

difference for orthopyroxene)^{14),15)}. In both Wang *et al.*¹⁰⁾ and Yoshino *et al.*⁵⁾, water content in the upper mantle was inferred using FT-IR based water content calibration. When the estimates of water content based on different methods are used, the influence of the used method needs to be evaluated. The purpose of this paper is to report the results of conductivity measurements of hydrous and anhydrous orthopyroxene and revise the estimate of the water content of the upper mantle where the influence of different methods of water content measurements is evaluated.

Experimental

Samples. We used two orthopyroxene single-crystals from the Stuttgart region in Germany (sample A) and the Han Nuoba region in eastern China (sample B). The surface of the sample was fresh and had good crystal form without any evidence of major

alteration. The chemical composition of the sample is shown in Table 1. The iron content of these orthopyroxene samples ($\text{Fe}/(\text{Fe}+\text{Mg}+\text{Ca}) = 0.14$ and 0.18) is higher than a typical upper mantle orthopyroxene, but aluminium content (0.4 and 0.8 wt%) is in the lower end of typical upper mantle peridotites¹⁶⁾ (a correction will be made on the influence of iron content, when we apply the present results to the upper mantle). The crystallographic orientation was determined using electron-backscattered diffraction with an error less than 1°. Samples of single-crystal orthopyroxene with different crystal axes ([001], [010] and [100]) were cut into a disc of $\phi 1.6 \text{ mm} \times 0.4 \text{ mm}$ with an ultrasonic drill and diamond slice; then, the samples were cleaned with acetone, alcohol and deionized-distilled water in turn. The samples were baked for 48 h in a 473 K vacuum drying furnace to remove the adsorbed water on the surface of the samples.

The water content of the samples was determined using the Fourier-transform infrared (FT-IR) spectroscopy for double-polished samples with a thickness of ~120 μm . FT-IR spectra were measured at several points in a sample and for each point, 256 scans were made, and the average of several points was used to calculate the water content. The infrared spectra of orthopyroxene along the direction of the [001] crystallographic axis are shown in Fig. 1. We used the Paterson calibration¹⁷⁾ to determine the water content of the sample,

$$C_W = \frac{B_j}{150\xi} \int \frac{K(\nu)}{(3780 - \nu)} d\nu \quad [1]$$

where C_W is the molar concentration of hydroxyl (ppm wt% H₂O or H/10⁶ Si), B_j is the density factor (2808 wt% or $3.11 \times 10^4 \text{ cmH}/10^6 \text{ Si}$), ξ is the orientation factor (1/2) and $K(\nu)$ is the absorption coefficient (cm⁻¹) at the wavenumber of ν . For orthopyroxene, FT-IR (Paterson) calibration and the SIMS (secondary ion mass spectrometry) measurements give nearly identical results¹⁴⁾. The integration was performed for the wavenumber ranging from 3000 to 3700 cm⁻¹. We obtained a water content of 4650 H/10⁶ Si (0.042 wt%) and less than 8 H/10⁶ Si

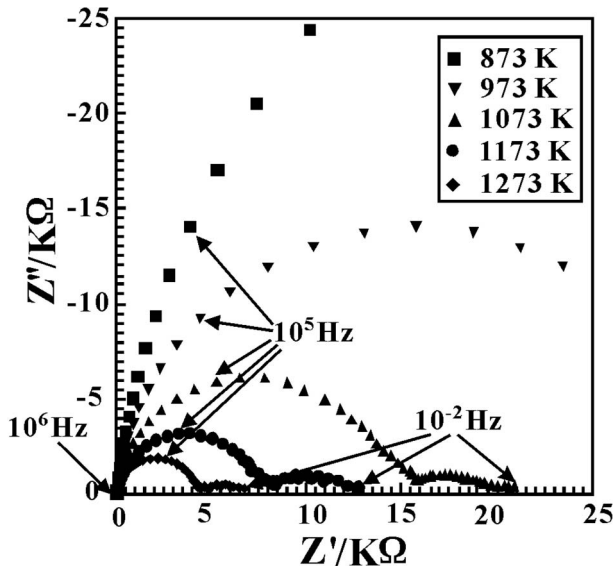


Fig. 2. Impedance spectra along the [001] crystallographic axis of a hydrous orthopyroxene from 10^{-2} to 10^6 Hz (right to left), obtained under conditions of 8.0 GPa, 873–1273 K, Mo–MoO₂ oxygen buffers and 0.042 wt% water content (Z' and Z'' stand for the real and imaginary parts of complex impedance, respectively).

(0.000072 wt%) for the orthopyroxene from the Stuttgart region in Germany and the Han Nuoba region in eastern China, respectively. Note that the latter value is close to the detection limit of water by FT-IR and should be considered as the upper limit. The water content was measured both before and after the conductivity measurements. The water loss during electrical conductivity measurement was less than 10%.

We also conducted Raman spectrum analysis before and after the electrical conductivity experiment. The results showed that there was no phase transition during the experiment.

Experimental methods. The experimental procedures are the same as those in the previous studies in our laboratory^{7)–10)} and therefore only the essence is described here. We used a Kawai-type multi-anvil press and used the Solartron-1260 Impedance/Gain-Phase analyzer to determine the conductivity from the impedance spectroscopy. The pressure was determined based on the separate calibrations using the phase transformations of some standard materials such as olivine-wadsleyite¹⁸⁾ and the phase transition of the coesite-stishovite transformation¹⁹⁾. The error in pressure estimate is ± 0.5 GPa. Temperature was

measured by a W₉₅Re₅–W₇₄Re₂₆ thermocouple. The error of the measured temperature was less than ± 10 K. Both the MgO pressure medium and the zirconia tube were baked for 10 h in a 1273 K furnace to avoid the effects of adsorbed water on the experimental results of the conductivity measurements. To control the oxygen fugacity and to avoid electric noise in the sample cavity from the heater, a 0.025 mm thick Mo foil was placed between the samples and the MgO insulation. A disc-shaped sample ($\phi 1.6$ mm \times 0.4 mm) was placed between two Mo electrodes ($\phi 0.5$ mm \times 0.3 mm).

Pressure was first raised at a rate of 2.0 GPa/h to the predetermined value of 8.0 GPa. After the desired pressure was reached, temperature was raised at a rate of 95 K/min to the designated value. After pressure and temperature are at the desired values, we run the ZPlot software of the Solartron-1260 Impedance/Gain-Phase analyzer to obtain the impedance spectra of the samples. The frequency range and signal voltage were 10^{-2} – 10^6 Hz and 300 mV, respectively. Conductivity was measured at temperature from 873 to 1473 K. In order to evaluate the possible influence of non-equilibrium effects, we measured the impedance spectra both with increasing and with decreasing the temperature. We did not see any appreciable hysteresis and conclude that the measured impedance corresponds to the equilibrium value.

Results and discussions

Results and comparison to other minerals.

The typical impedance spectra are shown in Fig. 2. Results from other crystallographic axes were similar to those that are illustrated. In the frequency range from 10^{-2} to 10^6 Hz, two impedance arcs were observed which correspond to two different conduction mechanisms: the circle at high frequencies corresponds to the grain interior conduction and the arc at lower frequencies corresponds to the polarization process at the sample and the electrode or at grain boundaries^{20),21)}. We determined the DC conductivity of a sample using high frequency part of spectra. The importance of using this part of spectra was discussed by previous papers^{8),9),11)} and will not be repeated here.

We calculated the conductivity of the sample from the measured resistivity using the formula, $\sigma = \frac{L}{SR}$, where σ is conductivity, L is sample thickness and S is the cross sectional area of the electrode.

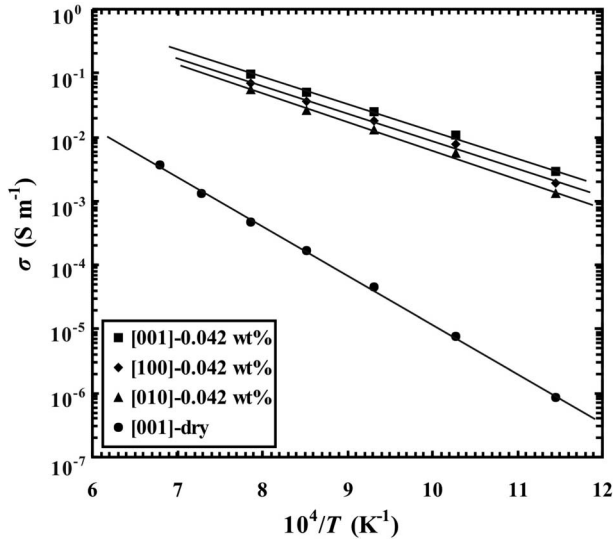


Fig. 3. Temperature dependence of electrical conductivity of a hydrous orthopyroxene (~ 4700 ppm H/Si) and an anhydrous (< 10 ppm H/Si) orthopyroxene at pressure of 8 GPa.

Figure 3 shows the relationship between electrical conductivity and temperature for these two samples. The data for each sample can be fitted to the following Arrhenius relation,

$$\sigma = \sigma_0 e^{-H^*/RT} \quad [2]$$

where σ_0 is the pre-exponential factor that is independent of the temperature and includes the water content's influence on the electrical conductivity, R is the ideal gas constant, H^* is the activation enthalpy and T is the absolute temperature. The Arrhenius fitting parameters for the hydrous and anhydrous electrical conductivity along the three different crystallographic axis directions are listed in Table 2. The anisotropy in conductivity is small.

For each sample (“dry” and “wet”), the electrical conductivity is well described by the Arrhenius relation with a single activation enthalpy for each, but the conductivity of a “wet” sample is much higher than that of a “dry” sample. This suggests that a single mechanism of conduction operates in each sample under these experimental conditions. However, the electrical conductivity of a sample with high water content is much higher than that of a water-poor (“dry”) sample, and the activation enthalpy is different. However, in order to evaluate the influence of water, it is necessary to compare the electrical conductivity with the same major element composition. Figure 4 shows a comparison of electrical

conductivities of olivine, orthopyroxene and pyrope garnet for the same Mg#⁷⁻¹⁰) at 8 GPa for the oxygen fugacity controlled by Mo-MoO₂, and either for the water content of 0.042 wt% or water-free conditions. The electrical conductivities of these minerals are remarkably similar: under these normalized conditions they agree within an order of magnitude, and the activation enthalpies are also similar (the influence of aluminum content is small²²). Consequently, we consider that the mechanisms of electrical conduction in orthopyroxene is similar to those in other minerals, namely, “polaron” conduction (conduction by hopping of electron between ferric and ferrous iron) under “dry” conditions and proton conduction under “wet” conditions. We also note that the electrical conductivity of our “dry” sample is similar to the conductivity reported in some of the previous studies^{23,24}. However, our results on “dry” sample are considerably different from those by Duba *et al.*²⁵ and by Hinze *et al.*²⁶ Duba *et al.*²⁵ reported a large hysteresis indicating the influence of non-equilibrium processes such as the influence of adsorbed water. Transformation of orthoenstatite to protoenstatite that occurs at low pressures may also be responsible for such a hysteresis. However, such a hysteresis was not observed in our studies presumably because all the parts were dried before each experiment and sample assembly was annealed before the measurement. Hinze *et al.*²⁶ measured the conductivity at 1 GPa where orthoenstatite is stable. They reported considerably smaller activation enthalpy (and higher conductivity) for nominally “dry” orthopyroxene than the present results. Based on our experience^{7,27}, we suspect that their samples contain a large amount of water. However, the water content of their samples was not measured and it is not possible to resolve the cause of discrepancy convincingly.

Huebner *et al.*²²) investigated the influence of trivalent cations (Cr³⁺ or Al³⁺) on electrical conductivity of orthopyroxene. The magnitude of this effect is, however, much smaller than the effects of water (hydrogen). Therefore we believe that a small difference in these cation concentration between the two samples studied here has relatively minor effects.

Water content of the upper mantle. Given the new data on electrical conductivity of orthopyroxene, and the similarities in conduction behavior between orthopyroxene and other minerals, we propose that the electrical conductivity of orthopyroxene follows the same trend as other minerals, viz.,

Table 2. Parameters of Arrhenius equation, $\sigma = \sigma_0 e^{-H^*/RT}$ for the electrical conductivity of hydrous and anhydrous orthopyroxene under conditions of 8.0 GPa and Mo-MoO₂ oxygen buffer

Run No.	orientation	T (K)	Water content (H/10 ⁶ Si)		σ_0 (S m ⁻¹)	H^* (KJ mol ⁻¹)
			Before experiment	After experiment		
K713	[001]	873-1273	4660	4540	181 ± 10	80 ± 2
K720	[100]	873-1273	4690	4600	162 ± 13	82 ± 3
K794	[010]	873-1273	4700	4640	153 ± 9	85 ± 2
K795	[001]	873-1473	<8	<7	531 ± 15	147 ± 6

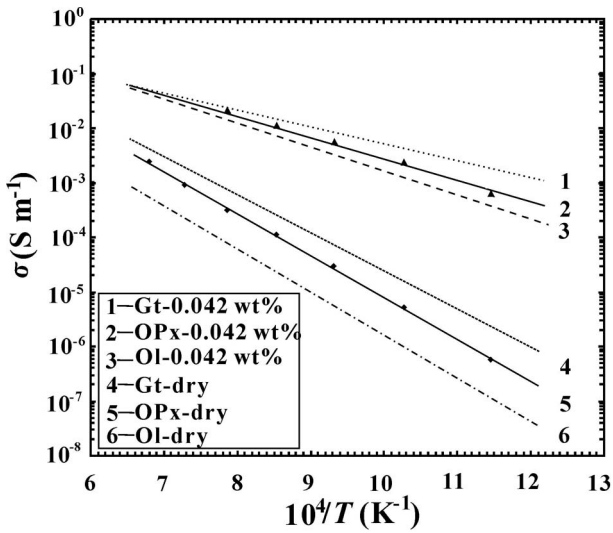


Fig. 4. A comparison of electrical conductivity of orthopyroxene with those of olivine^{10),50)} and pyrope-rich garnet⁹⁾ that are obtained at 8.0 GPa, 873-1473 K, Mo-MoO₂ oxygen buffer and the same iron content ($X_{Fe} = Fe/(Fe+Mg+Ca) = 0.10$). The results by Wang *et al.*¹⁰⁾ were corrected for Mo-MoO₂ buffer based on the results by Dai and Karato⁸⁾. The water content is measured using FT-IR. A correction is needed if the water content is measured by SIMS¹⁴⁾ (see text).

$$\sigma = A_1 \cdot \exp\left(-\frac{H_1^*}{RT}\right) + A_2 \cdot C_W^r \cdot \exp\left(-\frac{H_2^*}{RT}\right) \quad [3]$$

where the first term corresponds to the conductivity under “dry” (water-free) conditions, whereas the second term represents the conductivity under “wet” (water-rich) conditions. $A_{1,2}$ is corresponding pre-exponential term, $H_{1,2}^*$ activation enthalpy, C_W is the water content, and r is a non-dimensional constant. Although we did not determine, r , for orthopyroxene, using the analogy with other minerals, we assume $r = 0.62$, a value the same as olivine. Given the value of r , electrical conductivity of orthopyro-

xene is completely characterized. The parameters in such a relation for olivine, orthopyroxene and pyrope garnet are summarized in Table 3.

We use these relationships to estimate the water content of the asthenosphere by comparison of geophysically inferred conductivity values with mineral physics results on the influence of water on electrical conductivity. We assume that the asthenosphere has the pyrolite composition²⁸⁾, olivine : orthopyroxene : pyrope garnet = 60 : 25 : 15 (with $Mg/(Mg+Fe) = 0.88$) and calculate the electrical conductivity of pyrolite as a function of water content for a plausible range of asthenosphere temperature (1600 ± 100 K²⁹⁾). We consider a pressure of 5 GPa, but within the depth range of the asthenosphere (50–200 km), the influence of pressure on electrical conductivity for a given chemical composition (Fe content, water content) is negligibly small^{9),30)}.

An important issue in calculating the electrical conductivity is the partitioning of elements among co-existing minerals. When several minerals co-exist, then various elements will be partitioned among them and this effect must be included in the calculation of influence of water on the electrical conductivity of a mixture of minerals. Important elements for electrical conductivity are iron (Fe) and hydrogen (H). For iron partitioning, we used the results by Irfune and Isshiki³¹⁾ and made a small correction based on available experimental data³²⁾. Such a correction is more important for hydrogen. For hydrogen, the partition coefficients are calculated from the measured hydrogen solubility assuming the following relationship,

$$C_W^i = A^i f_{H_2O}^{r_i} \exp\left(-\frac{E_W^i + PV_W^i}{RT}\right) \quad [4]$$

where C_W^i is water content in mineral i , f_{H_2O} is the fugacity of water, r_i is a constant that depends on

Table 3. Electrical conductivity of upper mantle minerals (major element compositions are close to the typical upper mantle ($\text{Fe}/(\text{Fe}+\text{Mg}+\text{Ca}) = 0.10$ for olivine and orthopyroxene, $= 0.15$ for pyrope garnet). Parameters for the relation $\sigma = A_1 \cdot \exp\left(-\frac{H^*}{RT}\right) + A_2 \cdot C_W^r \cdot \exp\left(-\frac{H_2^*}{RT}\right)$ are shown corresponding to the Mo-MoO₂ buffer. The influence of Fe content is corrected by adjusting the pre-exponential factor (this effect may also be included as a variation in activation enthalpy). The results shown are from 4–8 GPa but pressure effects are small (less than $\sim 30\%$ in this pressure range). For olivine and pyrope garnet, the results are for isotropic polycrystalline aggregates. For orthopyroxene, the results are the average of single crystal data shown in Table 2. The results published by Wang *et al.*¹⁰⁾ are for the Ni-NiO buffer and are corrected for the Mo-MoO₂ buffer. Water content in these equations is for FT-IR based measurements. For olivine and garnet, a correction is needed if water content based on SIMS calibration is used (see text for detail)

	A_1 (S/m)	H_1^* (kJ/mol)	A_2 (S/m)	r	H_2^* (kJ/mol)
olivine	$10^{2.1}$	154	$10^{3.1}$	0.62	87
orthopyroxene	$10^{2.4}$	147	$10^{2.6}$	0.62	82
pyrope garnet	$10^{2.5}$	128	$10^{2.9}$	0.63	70

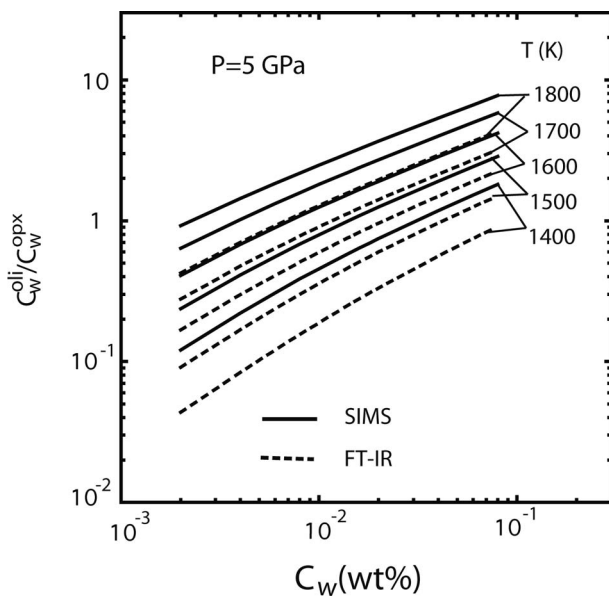


Fig. 5. Water (hydrogen) partitioning between olivine and orthopyroxene as a function of water content at 5 GPa.

$C_W^{oli,opx}$ is water content in olivine, orthopyroxene respectively and C_W is the total water content. The water partitioning depends strongly on the water content (water fugacity) and temperature. Water solubility data based on FT-IR and SIMS calibration are different for olivine leading to a difference in water partitioning.

the mechanisms of water dissolution, E_W^i and V_W^i are corresponding energy and volume change respectively. According to Mierdel *et al.*¹³⁾ and Kohlstedt *et al.*³³⁾, the water solubility in orthopyroxene and olivine depends on water fugacity differently ($r_i = 1$ for olivine³³⁾, $r_i = 0.5$ for Al-bearing orthopyrox-

ene¹³⁾), and consequently, the water partitioning between these two minerals depends on water fugacity as well as other thermodynamic parameter such as temperature. For pyrope garnet, there is no detailed experimental study on hydrogen solubility. We tentatively use the results by Mookherjee and Karato³⁴⁾ suggesting the similar dependence of hydrogen solubility on water fugacity as orthopyroxene. Mookherjee and Karato³⁴⁾ also show that water solubility in pyrope garnet is significantly smaller than that in Al-bearing orthopyroxene (by a factor of ~ 3). Because of the small volume fraction, pyrope garnet will occur in a pyrolite as isolated minerals, so the uncertainties on garnet conductivity will have only small effects on the results of electrical conductivity calculation. We calculated the water partition between olivine and orthopyroxene as a function of temperature and total water content assuming that the water content of garnet is 1/3 of that of orthopyroxene. We first calculated the water fugacity for a given total water content at a given pressure and temperature. Then the water content of each mineral was calculated using the solubility relationships.

Figure 5 shows the water (hydrogen) partition coefficient between olivine and orthopyroxene as a function of total water content (water fugacity) at 5 GPa and for various temperatures. Because the solubility data from Kohlstedt *et al.*³³⁾ is based on FT-IR and there is a factor of ~ 3 difference in water content measurements between FT-IR and SIMS (a factor of 3 larger water solubility than Kohlstedt *et al.*). Such a discrepancy is not observed for orthopyroxene¹⁴⁾ and wadsleyite. The cause of this discrepancy is not

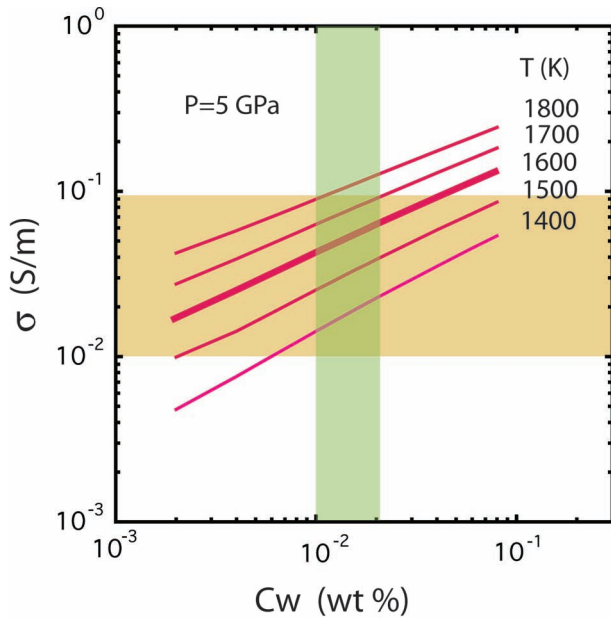


Fig. 6. Relationship between the electrical conductivity of a pyrolite upper mantle (olivine : orthopyroxene : garnet = 60 : 25 : 15, Mg# = 88) and the water content and temperature at 5 GPa.

SIMS-based water content is assumed. Different relationship will be obtained if FT-IR based water content is used. However, if the correction between FT-IR and SIMS-based water content (for olivine)¹⁴ is applied, the water content inferred from electrical conductivity will not be sensitive to the method of water content measurements. Orange region represents a typical range of electrical conductivity in the asthenosphere^{40,41,47}, and the green region corresponds to a range of water content in the asthenosphere inferred from petrological (geochemical) studies^{37–39}.

well known but it may be due to the influence of small water-filled inclusions that may be mineral specific. In any case, this SIMS versus FT-IR discrepancy for olivine is well documented^{14,15,35}, and we consider both cases. Water partitioning between olivine and orthopyroxene is strongly dependent on water content (water fugacity) and temperature because of the different dependence of water solubility on water fugacity and temperature for these minerals. A large fraction of water is dissolved in orthopyroxene for the low total water content and/or low temperature. The calculated results of partition coefficient depend on the method of water content measurement.

The electrical conductivity of a pyrolite was calculated using a model of electrical conductivity of a mixture. At a given conditions (temperature, pressure and water content), hydrogen partitioning among co-

existing minerals was calculated, and corresponding electrical conductivity of each mineral was calculated. Then the electrical conductivity of a mixture (pyrolite composition) is calculated. Several models for electrical conductivity of a mixture were proposed³⁶, but we use the Hashin-Shtrikman bounds. The choice of a model does not make much difference because the conductivity contrast is small (Hashin-Shtrikman upper and lower bounds give only less than a few % difference in electrical conductivity if the conductivity contrast is less than 2). In this calculation, we adjusted olivine data on electrical conductivity¹⁰ for SIMS-based water content. Therefore the water content in this figure corresponds to water content determined by SIMS. If FT-IR based water content is used, then the water content estimated from electrical conductivity should be interpreted as FT-IR based water content, and hence a factor of ~ 3 correction must be multiplied to olivine water content to convert it to SIMS-based water content. As far as such a conversion is made, water content inferred from electrical conductivity is not sensitive to the method of water content measurement.

The results of such calculations are shown in Fig. 6. For a plausible temperature of 1600 K for the asthenosphere²⁹, we obtain 0.04 wt% for a conductivity of 10^{-1} S/m and 0.01 wt% for 4×10^{-2} S/m. This is in good agreement with the petrological inference of water content for the MORB (mid-ocean ridge basalt) source region^{37–39} (0.01–0.02 wt%). However, there is a large regional variation in electrical conductivity of the asthenosphere exceeding more than a factor of $10^{40–42}$. If such a variation is attributed solely to the temperature variation, it would correspond to the variation in temperature of more than ~ 500 K that is not plausible in the asthenosphere⁴³. Consequently, we conclude that a large fraction of the lateral variation in electrical conductivity of the asthenosphere is caused by the variation in water content. Note that if we were to use the results by Yoshino *et al.*⁵ using SIMS-based water content calibration for olivine together with the present results for orthopyroxene, we would need a water content of ~ 0.1 wt% or more to explain the observed electrical conductivity. Such a value exceeds petrologically inferred water content (0.01–0.02 wt%). This is due to the inappropriate method used by Yoshino *et al.* including the use of a single, low frequency data at low temperatures as discussed by Karato and Dai^{8,11}.

What about partial melting? Partial melting is

often invoked to explain geophysical anomalies of the asthenosphere⁴⁴). However, as discussed by Shankland *et al.*⁴⁴) (see also Karato¹), it is difficult to attribute high electrical conductivity to partial melting because it would require a large volume of melt ($\sim 10\%$) for a basaltic melt. It is impossible to maintain such a large fraction of melt in a broad region of the asthenosphere because of the efficient compaction (the compaction length at the asthenospheric conditions is $\sim 10\text{--}100\text{ m}$ ⁴⁵). Recently, Gaillard *et al.*⁴⁶) showed that carbonatite melts have much higher electrical conductivity than hydrous basaltic melt and suggested that a small amount of carbonatite melt might explain high electrical conductivity of the asthenosphere. The high electrical conductivity in their carbonatite melts is essentially due to the high alkali content. The presence of such a melt cannot be ruled out, but in order for such a melt to explain high electrical conductivity, there must be a broad region where connected melt films (or tubes) are present. It is not clear how one can keep connected melt in a broad region against gravity-induced compaction.

In contrast, the present analysis showed that the geophysically inferred conductivity values of the asthenosphere, $10^{-2}\text{--}10^{-1}\text{ S/m}$, can be easily attributed to the solid-state mechanism by considering the role of water (hydrogen) in the asthenosphere with an amount that is consistent with the petrological model of the MORB source region. We conclude that partial melting is not required to explain high electrical conductivity of the asthenosphere. Note, however, that this does not imply that there is no partial melting in the asthenosphere. A small amount of partial melting could be present, but its effect is unlikely reflected in electrical conductivity.

One way to address the issue of partial melting versus water (hydrogen) explanation for the high conductivity of the asthenosphere is to investigate the regional variation of electrical conductivity. Partial melting hypothesis would imply higher conductivity in the asthenosphere of the central Pacific (near Hawaii) where hot materials are carried to the asthenosphere by a plume than in other typical oceanic asthenosphere. However, the published results show rather low electrical conductivity in the central Pacific (e.g., Utada *et al.*⁴⁷). Karato⁴⁸) proposed that the low electrical conductivity (and other geophysical anomalies) in the central Pacific may be due to water depletion in solid components caused by deep partial melting due to hot (and damp) plume.

However a limitation of this approach is the resolution of geophysical inference of electrical conductivity. Utada *et al.*⁴⁷) used relative long-period signals and their model for the upper mantle is poorly constrained. A detailed regional conductivity mapping of the upper mantle similar to the work by Kelbert *et al.*⁴⁹) will be helpful to resolve this issue.

Acknowledgements

We thank Professor Ikuo Kushiro, M.J.A., for kind handling of this paper. Mainak Mookherjee, Zhicheng Jing and Zhenting Jiang in Karato's laboratory kindly provided technical assistance. Professor Xingli Wang from Institute of Geochemistry, Chinese Academy of Sciences, China donated the single crystal orthopyroxene. This research was financially supported by the NSF of the United States (Grant No. 0608579) and the NSF of China (Grant No. 40704010).

References

- 1) Karato, S. (1990) The role of hydrogen in the electrical conductivity of the upper mantle. *Nature* **347**, 272–273.
- 2) Duba, A., Heard, H. C. and Schock, R. N. (1974) Electrical conductivity of olivine at high pressure and under controlled oxygen fugacity. *J. Geophys. Res.* **79**, 1667–1673.
- 3) Karato, S. (1974) MSc. Thesis. University of Tokyo, Tokyo, pp. 1–56.
- 4) Schock, R. N., Duba, A. G. and Shankland, T. J. (1989) Electrical conduction in olivine. *J. Geophys. Res.* **94**, 5829–5839.
- 5) Yoshino, T., Matsuzaki, T., Yamashita, S. and Katsura, T. (2006) Hydrous olivine unable to account for conductivity anomaly at the top of the asthenosphere. *Nature* **443**, 974–976.
- 6) Yoshino, T., Manthilake, G., Matsuzaki, T. and Katsura, T. (2008) Dry mantle transition zone inferred from the conductivity of wadsleyite and ringwoodite. *Nature* **451**, 326–329.
- 7) Huang, X., Xu, Y. and Karato, S. (2005) Water content of the mantle transition zone from the electrical conductivity of wadsleyite and ringwoodite. *Nature* **434**, 746–749.
- 8) Dai, L. and Karato, S. (2009) Electrical conductivity of wadsleyite under high pressures and temperatures. *Earth Planet. Sci. Lett.* **287**, 277–283.
- 9) Dai, L. and Karato, S. (2009) Electrical conductivity of pyrope-rich garnet at high temperature and pressure. *Phys. Earth Planet. Inter.* **176**, 83–88.
- 10) Wang, D., Mookherjee, M., Xu, Y. and Karato, S. (2006) The effect of water on the electrical conductivity in olivine. *Nature* **443**, 977–980.
- 11) Karato, S. and Dai, L. (2009) Comments on “Electrical conductivity of wadsleyite as a function of temperature and water content” by Manthilake *et al.* *Phys. Earth Planet. Inter.* **174**, 19–21.

- 12) Yoshino, T., Nishi, M., Matsuzaki, T., Yamazaki, D. and Katsura, T. (2008) Electrical conductivity of majorite garnet and its implications for electrical structure in the mantle transition zone. *Phy. Earth Planet. Inter.* **170**, 193–200.
- 13) Mierdel, K., Keppler, H., Smyth, J. R. and Langenhorst, F. (2007) Water solubility in aluminous orthopyroxene and the origin of Earth's asthenosphere. *Science* **315**, 364–368.
- 14) Aubaud, C., Withers, A. C., Hirschmann, M. H., Guan, Y., Leshin, L. A., Mackwell, S. J. and Bell, D. R. (2007) Intercalibration of FTIR and SIMS for hydrogen measurements in glasses and nominally anhydrous minerals. *Am. Miner.* **92**, 811–828.
- 15) Bell, D. R., Rossman, G. R., Maldener, J., Endisch, D. and Rauch, F. (2003) Hydroxide in olivine: A quantitative determination of the absolute amount and calibration of the IR spectrum. *J. Geophys. Res.* **108**, 10.1029/2001JB000679.
- 16) Pearson, D. G., Canil, D. and Shirey, S. B. (2003) Mantle samples included in volcanic rocks: Xenoliths and diamonds. *In* Treatise on Geochemistry (eds. Carlson, R. W., Holland, H. D. and Turekian, K. K.). Elsevier, Amsterdam, pp. 171–275.
- 17) Paterson, M. S. (1982) The determination of hydroxyl by infrared absorption in quartz, silicate glass and similar materials. *Bull. Miner.* **105**, 20–29.
- 18) Morishima, H., Kato, T., Suito, M., Ohtani, E., Urakawa, S., Utsumi, W., Shimomura, O. and Kikegawa, T. (1994) The phase-boundary between alpha-Mg₂SiO₄ and beta-Mg₂SiO₄ determined by in-situ X-ray observation. *Science* **265**, 1202–1203.
- 19) Zhang, J., Li, B., Utsumi, W. and Liebermann, R. C. (1996) In situ X-ray observations of the coesite-stishovite transition: reversed phase boundary and kinetics. *Phy. Chem. Miner.* **23**, 1–10.
- 20) Macdonald, J. R. (ed.) (1987) Impedance Spectroscopy. John Wiley & Sons, New York.
- 21) Roberts, J. and Tyburczy, J. A. (1991) Frequency dependent electrical properties of polycrystalline olivine compacts. *J. Geophys. Res.* **96**, 16205–16222.
- 22) Huebner, J. S., Wiggins, L. B. and Duba, A. G. (1979) Electrical conductivity of pyroxene which contains trivalent cations: Laboratory measurements and the lunar temperature profiles. *J. Geophys. Res.* **84**, 4652–4656.
- 23) Xu, Y. and Shankland, T. J. (1999) Electrical conductivity of orthopyroxene and its high pressure phases. *Geophys. Res. Lett.* **26**, 2645–2648.
- 24) Dai, L., Li, H., Liu, C., Shan, S. and Su, G. (2005) Experimental study on the electrical conductivity of orthopyroxene at high temperature and pressure under different oxygen fugacities. *Acta Geologica Sinica* **79**, 803–809.
- 25) Duba, A., Heard, H. C. and Schock, R. N. (1976) Electrical conductivity of orthopyroxene to 1400 °C and the resultant seleotherm. *In* Proc. Lunar Sci. Conf. 3173–3181.
- 26) Hinze, E., Will, G. and Cemi, L. (1981) Electrical conductivity measurements on synthetic olivines and an olivine, enstatite and diopside from Dreiser Weiher, Eifel (Germany) under defined thermodynamic activities as a function of temperature and pressure. *Phy. Earth Planet. Inter.* **25**, 245–254.
- 27) Nishihara, Y., Shinmei, T. and Karato, S. (2006) Grain-growth kinetics in wadsleyite: effects of chemical environment. *Phy. Earth Planet. Inter.* **154**, 30–43.
- 28) Ringwood, A. E. (1975) Composition and Structure of the Earth's Mantle. McGraw-Hill, New York.
- 29) McKenzie, D. and Bickle, M. J. (1988) The volume and composition of melt generated by extension of the lithosphere. *J. Petrol.* **29**, 625–679.
- 30) Xu, Y., Shankland, T. J. and Duba, A. G. (2000) Pressure effect on electrical conductivity of mantle olivine. *Phy. Earth Planet. Inter.* **118**, 149–161.
- 31) Irifune, T. and Isshiki, M. (1998) Iron partitioning in a pyrolite mantle and the nature of the 410-km seismic discontinuity. *Nature* **392**, 702–705.
- 32) Cemi, L., Will, G. and Hinze, E. (1980) Electrical conductivity measurements on olivines Mg₂SiO₄-Fe₂SiO₄ under defined thermodynamic conditions. *Physics Chem. Miner.* **6**, 95–107.
- 33) Kohlstedt, D. L., Keppler, H. and Rubie, D. C. Solubility of water in the α , β and γ phases of (Mg,Fe)₂-SiO₄. *Contributions to Miner. Petrol.* **123**, 345–357 (1996).
- 34) Mookherjee, M. and Karato, S. (2009) Solubility of water in pyrope-rich garnet at high pressure and temperature. *Geophys. Res. Lett.* (in press).
- 35) Koga, K., Hauri, E. H., Hirschmann, M. M. and Bell, D. R. (2003) Hydrogen concentration and analyses using SIMS and FTIR: Comparison and calibration for nominally anhydrous minerals. *Geophys. Geosyst.* **4**, 10.1029/2002GC000378.
- 36) McLachlan, D. S., Blaszkiewicz, M. and Newnham, R. E. (1990) Electrical resistivity of composite. *J. Am. Ceram. Soc.* **73**, 2187–2203.
- 37) Ito, E., Harris, D. M. and Anderson, A. T. (1983) Alteration of oceanic crust and geologic cycling of chlorine and water. *Geochem. Cosmochem. Acta* **47**, 1613–1624.
- 38) Dixon, J. E., Leist, L., Langmuir, J. and Schilling, J. G. (2002) Recycled dehydrated lithosphere observed in plume-influenced mid-ocean-ridge basalt. *Nature* **420**, 385–389.
- 39) Hirschmann, M. M. (2006) Water, melting, and the deep Earth H₂O cycle. *Annual Review of Earth Planet. Sci.* **34**, 629–653.
- 40) Baba, K., Chave, A. D., Evans, R. L., Hirth, G. and Randall, L. (2006) Electrical structure beneath the northern MELT line on the East Pacific Rise at 15°45'S. *Geophys. Res. Lett.* **33**, 10.1029/2006GL027528.
- 41) Ichiki, M., Baba, K., Obayashi, M. and Utada, H. (2006) Water content and geotherm in the upper mantle above the stagnant slab: Interpretation of electrical conductivity and seismic P-wave velocity models. *Phys. Earth Planet. Inter.* **155**, 1–15.
- 42) Baba, K., Utada, H., Goto, T., Kasaya, T., Shiizu, H. and Tada, N. (2009) Electrical conductivity imaging of the Philippine Sea upper mantle using sea-floor magnetotelluric data. *Phys. Earth Planet. Inter.* (in press).

- 43) McKenzie, D., Jackson, J. A. and Priestley, K. (2005) Thermal structure of oceanic and continental lithosphere. *Earth Planet. Sci. Lett.* **233**, 337–349.
- 44) Shankland, T. J., O'Connell, R. J. and Waff, H. S. (1981) Geophysical constraints on partial melt in the upper mantle. *Rev. Geophys. Space Phys.* **19**, 394–406.
- 45) Schubert, G., Turcotte, D. L. and Olson, P. (2001) *Mantle Convection in the Earth and Planets*, Cambridge University Press, Cambridge.
- 46) Gaillard, F., Malki, M., Iacono-Maziano, G., Pichavant, M. and Scaillet, B. (2008) Small amount of carbonatite melts explains high electrical conductivity in the asthenosphere. *Science* **322**, 1363–1365.
- 47) Utada, H., Koyama, T., Shimizu, H. and Chave, A. D. (2003) A semi-global reference model for electrical conductivity in the mid-mantle beneath the north Pacific region. *Geophys. Res. Lett.* **30**, 10.1029/2002GL016092.
- 48) Karato, S. (2008) Insights into the nature of plume-asthenosphere interaction from central Pacific geophysical anomalies *Earth Planet. Sci. Lett.* **274**, 234–240.
- 49) Kelbert, A., Schultz, A. and Egbert, G. (2009) Global electromagnetic induction constraints on transition-zone water content variations. *Nature* **460**, 1003–1006.
- 50) Xu, Y., Poe, B. T., Shankland, T. J. and Rubie, D. C. (1998) Electrical conductivity of olivine, wadsleyite, and ringwoodite under upper-mantle conditions. *Science* **280**, 1415–1418.

(Received Oct. 13, 2009; accepted Nov. 19, 2009)